Low-energy (p,γ) reactions in Ni and Cu nuclei using a microscopic optical model

G. Gangopadhyay
Department of Physics, University of Calcutta 92, Acharya Prafulla Chandra Road, Kolkata 700 009, India
(Received 22 June 2010; revised manuscript received 13 July 2010; published 26 August 2010)

Radiative capture reactions for low-energy protons have been theoretically studied for Ni and Cu isotopes using the microscopic optical model. The optical potential has been obtained in the folding model using different microscopic interactions with the nuclear densities from relativistic mean field calculations. The calculated total cross sections as well as the cross sections for individually low-lying levels have been compared with measurements involving stable nuclear targets. Rates for the rapid proton capture process have been evaluated for astrophysically important reactions.

DOI: 10.1103/PhysRevC.82.027603 PACS number(s): 25.40.Lw, 24.10.Ht, 27.40.+z, 27.50.+e

Optical model potentials constructed utilizing microscopic densities from standard nuclear models have proved to be very successful in describing low-energy nuclear reactions. Elastic scattering calculations using such potentials have been able to explain the observed cross sections even in nuclei far off the stability valley. Low-energy projectiles probe only the outermost part of the target nuclei. Hence the nuclear skin plays a very important role in such reactions. Theoretical models can provide a good description of the density profile and are capable of producing excellent estimates of reaction cross sections. Alternatively, the ability of different models to reproduce the nuclear density profile may be compared in their ability to predict reaction cross sections.

Proton capture reactions at low energy are important to understand the astrophysical rp process. At energies below the Coulomb barrier, the cross sections are small. However, as the Gamow window lies entirely below the barrier, estimation of the cross section below the barrier is of crucial importance. We note that capture may lead to the ground state, to the excited states, or to the continuum of the compound nucleus.

The relativistic mean field (RMF) approach is now a standard tool in low-energy nuclear structure. It has been able to explain different features of stable and exotic nuclei such as ground state binding energy, deformation, radius, excited states, spin-orbit splitting, and neutron halo [1]. RMF is known to provide a good description of various features in the $A = 60$ mass region (see Ref. [2], and references therein). There are different variations of the Lagrangian density as well as a number of different parametrizations. In this Brief Report, we have employed three such densities, NL3 [3], TM1 [4], and FSU Gold [5], to study (p,γ) reactions in stable Ni and Cu nuclei. The NL3 density contains, apart from the usual terms for a nucleon meson system, nonlinear terms involving self-coupling of the scalar-isoscalar meson. The TM1 density includes additional terms describing self-coupling of the vector-isoscalar meson. The FSU Gold density includes coupling between the vector-isoscalar meson and the vector-isovector meson as well. We note that results of our cross-sectional calculation for all three Lagrangian densities are practically identical and present the results for FSU Gold only.

In the conventional RMF + BCS approach, the equations obtained are solved under the assumptions of classical meson fields, time reversal symmetry, no-sea contribution, and so on. Pairing is introduced under the BCS approximation. Usually the resulting equations are solved on a harmonic oscillator basis [6]. However, because we need the densities in coordinate space, a solution of the Dirac and Klein-Gordon equations in coordinate space has been preferred. This approach has earlier been used [2,7,8] to study neutron-rich nuclei in different mass regions. We have found that the present method describes the properties of the nuclei with $Z = 28$ equally well as the more involved relativistic Hartree-Bogoliubov approach. In the second and third columns of Table I, we compare the results for the binding energy values for the stable isotopes for FSU Gold. The valence neutron-proton correlation correction has been taken care of following the prescription of Ref. [11]. Much more important from the point of view of the density profile are the next two columns, in which we compare the measured charge radii (r_{ch}) with theory. The latter values have been obtained from the point proton distribution (r_p) using the simple prescription $r_{ch} = (r_p^2 + 0.64)^{1/2}$, with all quantities given in femtometers. The results show that RMF can describe the ground state of these nuclei with sufficient accuracy.

The optical model potentials for the reactions are obtained using two effective interactions derived from the nuclear matter calculation in the local density approximation, that is, by substituting the nuclear matter density with the density distribution of the finite nucleus. Thus the microscopic nuclear potentials have been obtained by folding the effective interactions with the microscopic densities from the RMF calculation. The Coulomb potentials have been similarly generated by folding the Coulomb interaction with the microscopic proton densities. We have already used such potentials to calculate lifetimes for proton, alpha, and cluster radioactivity [12] as well as elastic proton scattering [7] in different mass regions of the periodic table.

One of the interactions chosen in this Brief Report is the interaction of Jeukenne, Lejeune, and Mahaux (JLM) [13], in which further improvement is incorporated in terms of the finite range of the effective interaction by including a Gaussian form factor. We have used the global parameters for the effective interaction and the respective default normalizations for the potential components from Refs. [14,15], with Gaussian range values of $t_{\rm real} = 1.25$ fm and $t_{\rm imag} = 1.35$ fm.

TABLE I. Experimental binding energies [9] and radii [10] compared with calculated values for the FSU Gold Lagrangian density. The $G_{\rm norm}$ values used in different isotopes are also indicated in the last two columns. See text for details.

	Binding energies (MeV)		r_{ch} (fm)		$G_{\rm norm}$	
	Experimental	Theoretical	Experimental	Theoretical	JLM	DDM3Y
^{58}Ni	506.46	508.83	3.775	3.751	0.85	0.85
^{60}Ni	526.84	527.50	3.812	3.779	0.60	0.60
^{61}Ni	534.66	535.05	3.822	3.792	0.70	0.70
^{62}Ni	545.26	544.71	3.841	2.828	0.60	0.60
^{64}Ni	561.76	561.97	3.859	3.827	0.95	0.80
^{63}Cu	551.38	551.17	3.883	3.848	0.55	0.55
^{65}Cu	569.21	569.43	3.902	3.866	0.95	0.95

We have also used the density-dependent interaction DDM3Y [16,17] in this Brief Report. This was obtained from a finite-range energy-independent M3Y interaction by adding a zero-range energy-dependent pseudopotential and introducing a density-dependent factor. This interaction has been employed widely in the study of nucleon-nucleus as well as nucleus-nucleus scattering, calculation of proton radioactivity, and so on. The density dependence has been chosen in the form $C(1-\beta\rho^{2/3})$ [17]. The constants were obtained from nuclear matter calculation [18] as $C = 2.07$ and $\beta = 1.624$ fm^2. For scattering, we have taken real and imaginary parts of the potential as 0.9 times and 0.1 times the DDM3Y potential, respectively.

The reaction calculations have been performed with the computer code TALYS 1.2 [19], assuming spherical symmetry for the target nuclei. The DDM3Y interaction is not a standard part of TALYS but can easily be incorporated. Because nuclear matter–nucleon potential does not include a spin-orbit term, the TALYS 1.2 code obtains the spin-orbit potential from the Scheerbaum prescription [20] coupled with the phenomenological complex potential depths λ_{vso} and λ_{wso}:

$$U^{so}_{n(p)}(r) = (\lambda_{vso} + i\lambda_{wso})\frac{1}{r}\frac{d}{dr}\left[\frac{2}{3}\rho_{p(n)} + \frac{1}{3}\rho_{n(p)}\right]. \quad (1)$$

The depths are functions of energy, given by $\lambda_{vso} = 130\exp(-0.013E) + 40$ and $\lambda_{wso} = -0.2(E-20)$, with E in MeV. This has been used in the calculations of both the interactions.

The TALYS code has a number of features useful to study reactions. We have employed the full Hauser-Feshbach calculation with transmission coefficients averaged over total angular momentum values and with corrections from width fluctuations. Hilaire's microscopic level density values included in the code have been used, though we have confirmed that the results are not substantially modified if a different level density formula is assumed. Up to 25 discrete levels of the compound nucleus have been included in the calculation. The γ-ray strength has been calculated in the Hartree-Fock-Bogoliubov model. However, we find that though the trends have been correctly reproduced in all the cases, the actual values of the cross sections are often overpredicted. Thus the γ-ray strength was visually normalized to match with the experimentally observed cross sections using the parameter $G_{\rm norm}$ in the code, though no fit was performed. In the last two columns of Table I, we tabulate the values of this parameter used for the different targets. We should also mention that in the case of ^{60,61}Ni, the experimental values from different measurements differ by a large amount, and we have chosen the latest measurements to determine $G_{\rm norm}$.

In Fig. 1, we have compared our results with various experimental measurements in Ni isotopes and have found reasonable agreement. In Fig. 2, we present the results for stable Cu isotopes. As the astrophysically important Gamow

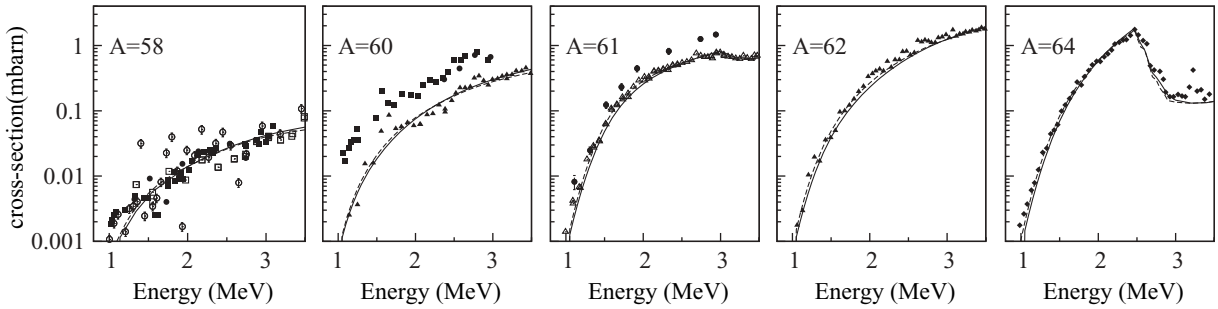

FIG. 1. Cross sections for (p,γ) reactions in stable Ni isotopes. The mass numbers of the target nuclei are indicated. The data are from Refs. [21] (open squares), [22] (filled squares), [23] (filled circles), [24] (open circles), [25] (filled triangles), [26] (open triangles), and [27] (diamonds). The solid and dashed lines refer to results for JLM and DDM3Y interactions, respectively.

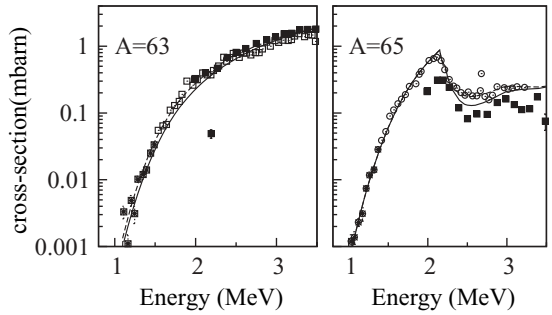

FIG. 2. Cross sections for (p,γ) reactions in stable Cu isotopes. The data are from Refs. [27] (open squares), [28] (filled squares), and [29] (open circles). See Fig. 1 for details.

window lies in the region 1.1–3.3 MeV for these nuclei, we compare the results up to 3.5 MeV proton energy. As already mentioned, $G_{\rm norm}$ is the only parameter that we have modified to normalize the experimental data. All other parameters in the Lagrangian density and the interaction are standard and have not been changed. The DDM3Y and JLM interactions perform almost identically in almost all nuclei. The former sometimes appears to produce slightly better results, but in view of the large disagreement between different measurements, this conclusion remains very tentative. We see that our calculation can explain cross-sectional values ranging over 3 orders of magnitude and also beyond the neutron evaporation threshold. We note here that the default local and global optical potentials [30] in the TALYS package also can be used with suitable normalization of γ-ray strength to produce comparable results for certain energy ranges. For example, with $G_{\rm norm} = 0.5$, the results for the low-energy values for DDM3Y and results using the default potentials are nearly identical in the ^{64}Ni(p,γ) reaction, but above the neutron evaporation threshold, the predictions by the default potentials, using the same $G_{\rm norm}$ value, are definitely poorer compared to those of the microscopic calculations.

The cross sections corresponding to the different low-lying levels of the compound nucleus have been measured in some of the preceding reactions. In Fig. 3, we show the results for the ground state and the first two excited states in the

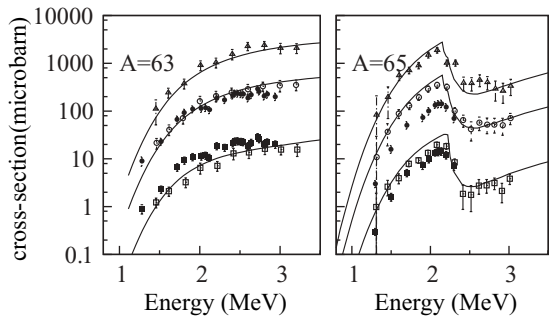

FIG. 3. Partial cross sections for ^{63,65}Cu(p,γ) reactions to the low-lying states in ^{64,66}Zn. Open (filled) symbols refer to data from Ref. [31] (Ref. [32]). Squares, circles, and triangles represent data for transition to the ground state and to the first excited state (multiplied by 10) and the second excited state (multiplied by 100), respectively. The mass numbers of the target nuclei are indicated.

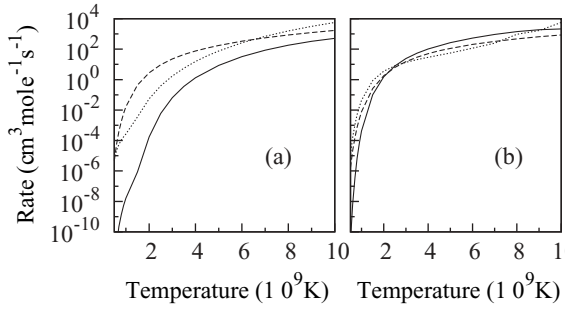

FIG. 4. Astrophysical proton capture rates in (a) ^{56}Ni and (b) ^{57}Cu given by the present work (solid line), NON-SMOKER calculation [34] (dashed line), and shell model results [35] (dotted line).

^{63,65}Cu$(p,\gamma)^{64,66}$Zn reactions using the inputs of the TALYS 1.2 code and the corresponding experimental measurements. Similar agreements are also observed in Ni isotopes. The results are for the JLM interaction only. The DDM3Y results are nearly identical. We may conclude that the present method is suitable to describe the proton capture cross section by stable Ni and Cu isotopes.

With the success of the present approach, we have employed it to calculate the astrophysical rapid proton capture rate in Ni and Cu nuclei. Nucleosynthesis theories [33] suggest that the preceding process is very important in ^{56}Ni and ^{57}Cu, for which we present our results in Fig. 4. Because the laboratory cross sections are not available for the two unstable targets, we have assumed $G_{\rm norm} = 1$. We also compare our results with two theoretical calculations based on the Hauser-Feshbach formalism code NON-SMOKER [34] and the shell model [35], respectively. The stellar enhancement factor has not been incorporated in the results. The results for the DDM3Y interaction are nearly identical and have not been plotted. We note that there are substantial differences between the three calculations in the case of ^{58}Ni; in particular, the NON-SMOKER results are much larger compared to the present results. We find that the cross sections from the NON-SMOKER code [34] are very much larger than experimental measurements as one goes to proton-rich Ni isotopes. Thus we may expect the astrophysical rates from Ref. [34] to be greater in ^{56}Ni.

In summary, cross sections for low-energy (p,γ) reactions for stable Ni and Cu nuclei have been calculated using the TALYS code. The microscopic optical potential has been obtained by folding two different microscopic interactions, JLM and DDM3Y, with the densities of the target nuclei obtained from three different RMF Lagrangian densities, namely, NL3, TM1, and FSU Gold. Astrophysical rates for the rp process have been calculated and compared with standard calculations in two important nuclei: ^{56}Ni and ^{57}Cu.

This work has been carried out with financial assistance of the UGC-sponsored DRS Programme of the Department of Physics of the University of Calcutta. The author gratefully acknowledges the hospitality of the ICTP, Trieste, where a part of the work was carried out.

[1] P. Ring, Prog. Part. Nucl. Phys. **37**, 193 (1996).
[2] M. Bhattacharya and G. Gangopadhyay, Phys. Rev. C **72**, 044318 (2005); Fizika (Zagreb) **16**, 113 (2007).
[3] G. A. Lalazissis, J. König, and P. Ring, Phys. Rev. C **55**, 540 (1997).
[4] Y. Sugahara and H. Toki, Nucl. Phys. A **579**, 557 (1994).
[5] B. G. Todd-Rutel and J. Piekarewicz, Phys. Rev. Lett. **95**, 122501 (2005).
[6] Y. K. Gambhir, P. Ring, and A. Thimet, Ann. Phys. (NY) **198**, 132 (1990).
[7] G. Gangopadhyay and S. Roy, J. Phys. G **31**, 1111 (2005).
[8] M. Bhattacharya and G. Gangopadhyay, Phys. Rev. C **75**, 017301 (2007).
[9] G. Audi, A. H. Wapstra, and C. Thibault, Nucl. Phys. A **729**, 337 (2003).
[10] I. Angeli, At. Data Nucl. Data Tables **87**, 185 (2004).
[11] M. Bhattacharya and G. Gangopadhyay, Phys. Lett. B **672**, 182 (2009); G. Gangopadhyay, J. Phys. G **37**, 015108 (2010).
[12] G. Gangopadhyay, J. Phys. G **36**, 095105 (2009).
[13] J. P. Jeukenne, A. Lejeune, and C. Mahaux, Phys. Rev. C **10**, 1391 (1974).
[14] [http://www-nds.iaea.org/ripl2].
[15] E. Bauge, J. P. Delaroche, and M. Girod, Phys. Rev. C **63**, 024607 (2001).
[16] A. M. Kobos, B. A. Brown, R. Lindsay, and G. R. Satchler, Nucl. Phys. A **425**, 205 (1984).
[17] A. K. Chaudhuri, Nucl. Phys. A **449**, 243 (1986); **459**, 417 (1986).
[18] D. N. Basu, J. Phys. G **30**, B7 (2004).
[19] A. J. Koning, S. Hilaire, and M. Duijvestijn, in *Proceedings of the International Conference on Nuclear Data for Science and Technology*, edited by O. Bersillon, F. Gunsing, E. Bauge, R. Jacqmin, and S. Leray (Nice, France, 2008), pp. 211–214.
[20] R. R. Scheerbaum, Nucl. Phys. A **257**, 77 (1976).
[21] C. W. Tingwell, L. W. Mitchell, M. E. Sevior, and D. G. Sargood, Nucl. Phys. A **439**, 371 (1985).
[22] G. A. Krivonosov, O. I. Ekhichev, B. A. Nemashkalo, V. E. Storizhko, and V. K. Chirt, Izv. Akad. Nauk. SSSR, Ser. Fiz. **41**, 2196 (1977).
[23] G. A. Krivonosov, B. A. Nemashkalo, O. I. Ekhichev, A. P. Klucharev, A. I. Popov, V. E. Storizhko, and V. K. Chirt, in *Proceedings of the 24th Conference on Nuclear Spectroscopy and Nuclear Structure* (Kharkov, Ukraine, 1974), p. 352.
[24] C. W. Cheng and J. D. King, Can. J. Phys. **58**, 1677 (1980).
[25] C. I. W. Tingwell, V. Y. Hansper, S. G. Tims, A. F. Scott, A. J. Morton, and D. G. Sargood, Nucl. Phys. A **496**, 127 (1988).
[26] C. I. W. Tingwell, V. Y. Hansper, S. G. Tims, A. F. Scott, and D. G. Sargood, Nucl. Phys. A **480**, 162 (1988).
[27] M. E. Sevior, L. W. Mitchell, M. R. Anderson, C. W. Tingwell, and D. G. Sargood, Aust. J. Phys. **36**, 463 (1983).
[28] S. Qiang, Ph.D. thesis, University of Kentucky, 1990.
[29] B. A. Nemashkalo, Y. P. Mel'nik, V. E. Storizhko, and K. V. Shebeko, Yad. Fiz. **37**, 3 (1983).
[30] A. J. Koning and J. P. Delaroche, Nucl. Phys. A **713**, 231 (2003).
[31] B. A. Nemashkalo, S. N. Utenkov, S. S. Ratkevich, and I. D. Fedorets, Izv. Akad. Nauk. SSSR, Ser. Fiz. **67**, 1556 (2003).
[32] B. A. Nemashkalo, V. E. Storizhko, and V. K. Chirt, in *Proceedings of the 31st Conference on Nuclear Spectroscopy and Nuclear Structure* (Samarkand, Uzbekistan, 1981), p. 322.
[33] H. Schatz *et al.*, Phys. Rep. **294**, 167 (1998).
[34] T. Rauscher and F.-K. Thielmann, At. Data Nucl. Data Tables **75**, 1 (2000); **79**, 47 (2001).
[35] J. L. Fisker, V. Barnard, J. Jörres, K. Langanke, G. Martinez-Pinedo, and M. Wiescher, At. Data Nucl. Data Tables **79**, 241 (2001).